2. An Analysis of Ship Capsizing in Quartering Seas

by Masami Hamamoto*, *Member* Yoon Soo Kim**, *Member*
Akihiko Matsuda**, *Member* Hiroyuki Kotani**, *Member*

(*From J.S.N.A. Japan, Vol. 171, June 1992 and Vol. 172, Dec. 1992*)

Summary

This paper is concerned with the righting arm and capsizing of a ship in extreme quartering waves. The effects of wave height, wave length and heading angles of ship to waves on the righting arm are analytically investigated for a container ship. A time domain numerical simulation program for motions and capsizing has been used to investigate motions in a variety of wave configulations. Numerical simulations based on a mathematical model are carried out to find out the critical situation leading up to capsizing of a container ship in extreme quartering waves. Various phisical mechanism that could be responsible for capsize are pointed out by numerical experiments.

1. INTRODUCTION

Stability against capsizing[23,24,25,26,27,28] in extreme seas is one of the most fundamental requirements for the safety of ship at sea. At the same time it is one of the most complicated phenomena to investigate on the basis of analytical approach because the phenomena are concerned with extreme motion both of ship and waves. What is the dengerous situations leading up to capsizing of ship in extreme seas? For this problem, several investigators carried out model experiments[12] and pointed out capsize modes such as, resonant rolling mode in beam wind and waves, pure loss of stability at wave crest amidship[12], low cycle resonance due to parametric excitation[12], broaching-to due to successive waves[12,15,16], period bifurcation of rolling[26], surfriding phenomena [29], etc.

It is a big problem to investigate what is the essential indices or mechanism to bring a ship to capsize. As well as known, the metacentric height GM, righting arm GZ and its area are the traditional indices which, as pointed out by Paulling[5], vary with respect to the relative position of ship to waves. These indices are hydrostatic feature for stability. In order to make an analytical approach to the phenomena mentioned above, it is necessary to consider the dynamics of motion and capsizing for stability. The purpouse of this paper is to discuss the dynamics of motion by using a mathematical model to describe the ship motion and capsizing.

For a mathematical model to conduct numerical simulations, it is necessary to summarize the outline of ship motion, hydrostatic and hydrodynamic forces on ship. The frequency of wave encounter is low in following to quartering seas when a ship is running at high speed. As a result, the ship motions will be determined largely by the hydrostatic forces including Froude-Krylov forces which may be computed for the exact position of ship and waves, and the contribution of hydrodynamic forces will be relatively not so much. This enables us to retreat from the difficulty and necessity of determining the hydrodynamic forces with great accuracy taking into account the geometrical variation of the immersed hull during large amplitude motions.

According to the considerations mentioned above, we tried to drive a mathematical model taking into account the linearized hydrodynamic forces and non-linear hydrostatic forces which may be computed for

*Osaka University
**Graduate School of Osaka University

the exact immersed hull. Using this mathematical model, we conducted numerical experiments to analyze the ship motions and capsizing in extreme quartering seas.

2. ANALYSIS OF HYDROSTATIC STABILITY.

As pointed out by Paulling[5], for waves of length nearly equal to the ship length the righting arm GZ is increased at a wave trough near amidships and decreased at a crest near amidships. The variation of GZ in waves will affect the roll motion of the ship and play an important role in extreme motion and capsizing.

According to the coordinate system, the GZ[27] taking into account the exact position of ship and waves is given by

$$W \cdot GZ \cong -\rho g \int_L (y_{B(x)} \cos\phi - z_{B(x)} \sin\phi) A(x) \mathrm{d}x$$
$$-\rho g \sin\chi \int_L (z_{B(x)} \cos\phi + y_{B(x)} \sin\phi)$$
$$\times ak \frac{\sin(k\frac{B(x)}{2}\sin\chi)}{k\frac{B(x)}{2}\sin\chi} e^{-k\{\zeta_G + d(x)\}} \qquad (1)$$
$$\times A(x) \sin k(\xi_G + x\cos\chi - ct) \mathrm{d}x$$

where ρ is density of water, g acceleration of gravity, c phase speed of wave, t time, $B(x)$ ship breadth at draft, $A(x)$ submerged area, $y_{B(x)}$ and $z_{B(x)}$ are gravity center of submerged area. The first term of right side in Eq.(1) is stability of hydrostatic pressure gradient ρg and the second term is stability by lateral force of heading angle ψ of ship to wave.

In order to analyze the relationships between the GZ and the effect of following items:

- Effects of wave length to ship length ratio λ/L
- Effects of wave height to length ratio H/λ
- Effects of heading angle ψ of ship to wave
- Dynamical stability for the relative position of ship to wave

We used a container ship as shown in Fig.1. Fig.2 shows GZ curves of designed GM, J.G regulation at C=1 and IMO A.562 at C=1[19]

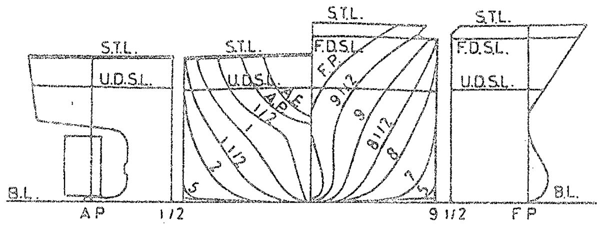

L=115.0(m) B=19.0(m) d=6.4(m) Δ=10135.0(ton)

Fig.1 Principal dimension

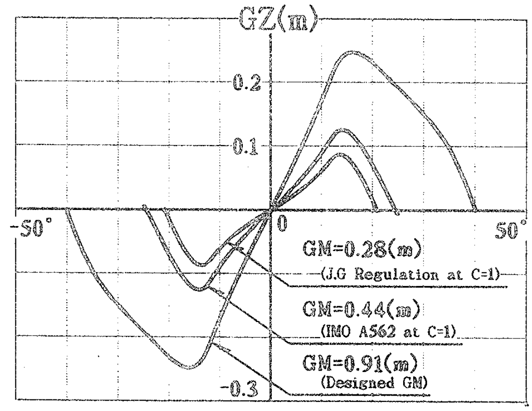

Fig.2 GZ curves in still water

<u>Effects of wave length to ship length ratio λ/L</u>

The righting arm GZ is remarkably reduced when the crest of a wave is about amidships and increased when the trough of a wave is about amidships. Such variations of GZ in a wave are related to the relative position of ship to waves and the wave length to ship length ratio. Fig.3 shows the variation of GZ with respect to the relative position ξ_G/λ of ship to waves and the wave length to ship length ratio λ/L. In this figure, ξ_G/λ is equal to 0 at the trough, 0.25 at the up slope, 0.5 at the crest and 0.75 at the down slope amidships. The variation is smaller for larger wave length at constant wave height. The maximum variation comes in the same length as ship.

<u>Effects of wave height to length ratio H/λ</u>

Fig.4 indicates the variations of GZ with respect to the wave height at constant wave length equal to the ship length. The variation is proportional to the wave height.

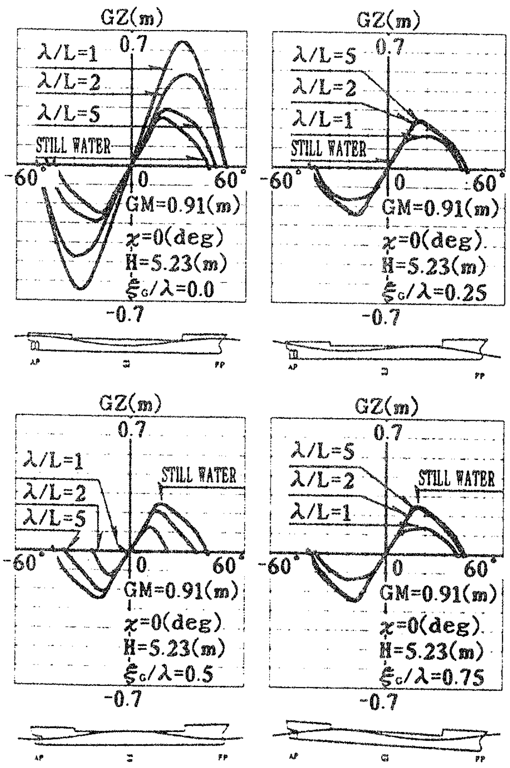

Fig.3 Variation of stability curves due to the ratio of wave length to ship length

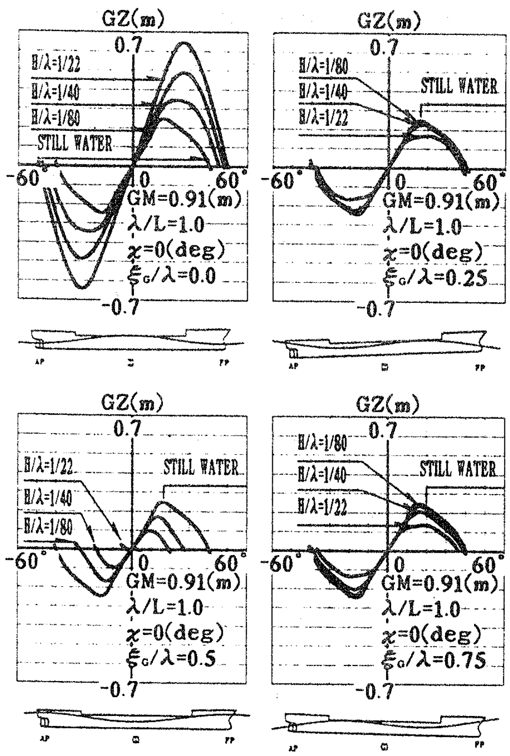

Fig.4 Variation of stability curves due to the ratio of wave height to length

Effects of heading angle ψ of ship to wave

Fig.5 indicates the variations of GZ with respect to the heading angle χ. The effect of heading angles on the GZ can be significant and the GZ in beam sea condition is about the same as that in still water. But the GZ is smaller for smaller heading angles and the smallest one is that in a following sea.

Dynamical stability for the relative position of ship to waves

The righting arm GZ vary with the relative position of ship to waves, heading angles, wave height and length. Accordingly the dynamical stability vary with the parameters mentioned above. Figs.6 and 7 show the variation of dynamic stability with respect to the relative position of ship to waves. In this case, the dynamical stability is the area of GZ at the vanishing angles of stability for $\lambda/L = 1.0$ and $\lambda/L = 1.5$.

$$E = W\int_0^{\phi_r} GZ(\phi)d\phi \qquad (2)$$

The dynamic stability takes the smallest one near wave crest and the largest one near wave trough. And then the dynamical stability is seen to be closely related to the capsize of ship in extreme following and quartering seas.

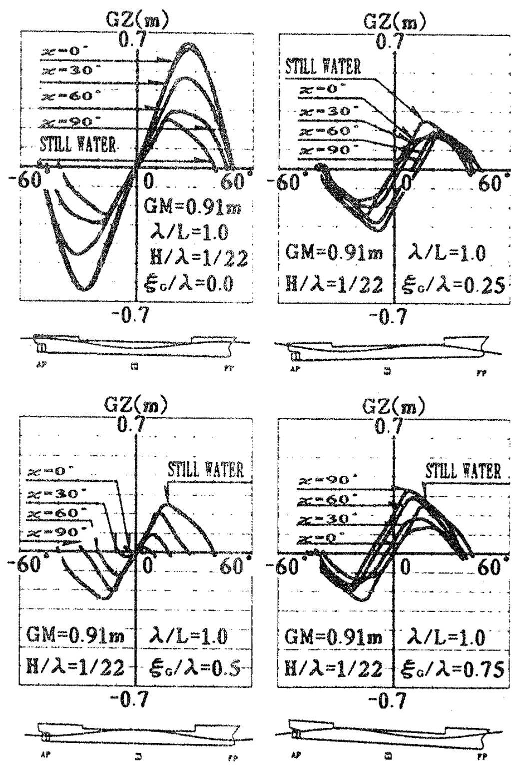

Fig.5 Variation of stability curves due to heading angle of ship to waves

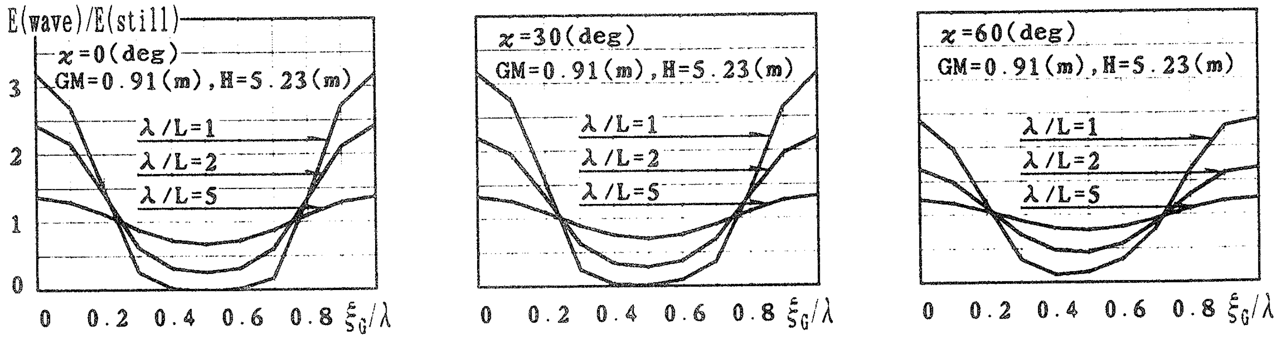

Fig.6 Variation of stability curves due to the relative position of ship to waves

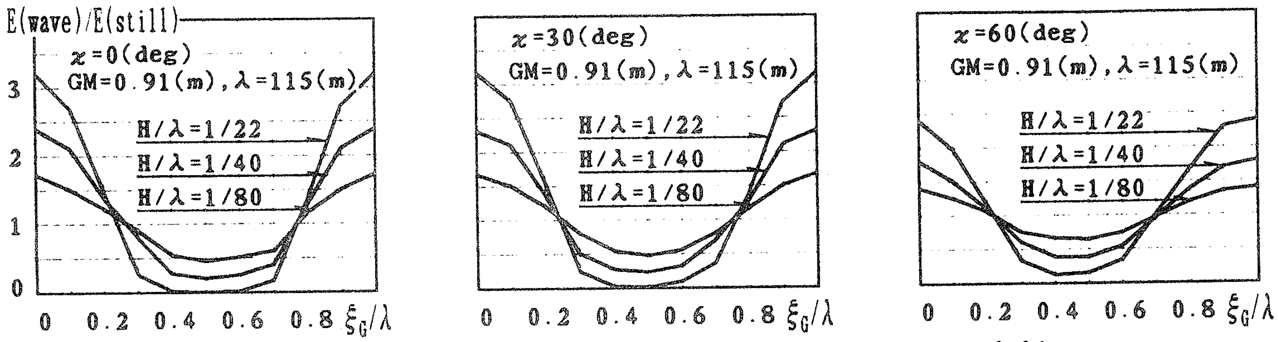

Fig.7 Variation of stability curves due to the relative position of ship to waves

3. A MATHEMATICAL MODEL FOR NUMERICAL EXPERIMENTS

We used the equations of motion with respect to a new coordinate system called Horizontal body axes[11,28] which have rotation about z' axis and no rotation about x' and y' axes but a ship is able to rotate about x' and y' axes as shown in Fig.8. The use of Horizontal body axes are reasonably simple and convenient for representing manoeuvring motion with large roll angles in horizontal plane and seakeeping motion with large roll angles in vertical plane, because horizontal and vertical forces on ship automatically include the effects of large heel and roll angles. According to this coordinate system, the equations of motion are derived in the following forms.

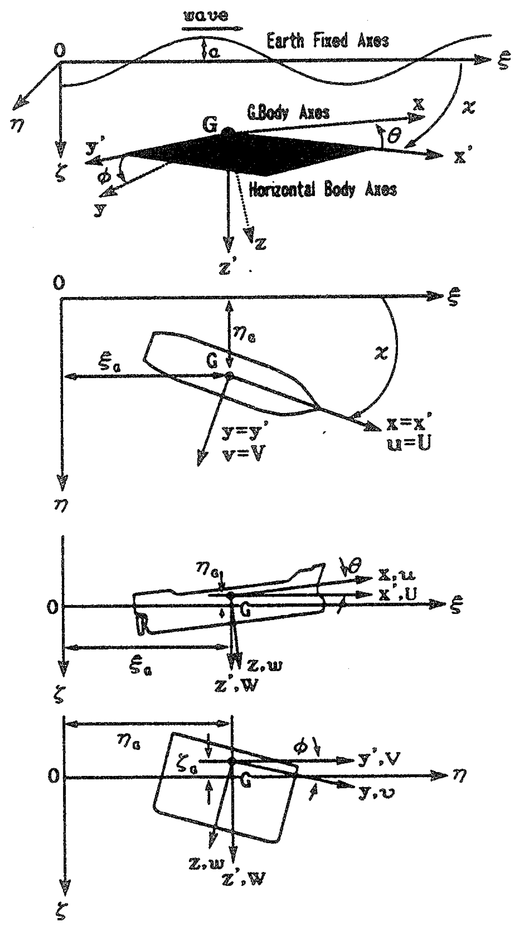

Fig.8 Coordinate systems

Translational Motions And Forces

$$\begin{aligned}(m+m_x)\dot{U} &- (m+m_y)V\dot{\psi} + X_{V\dot{\psi}}\,V\dot{\psi} \\ &+m_x z_G\ddot{\theta} + m_z\dot{\zeta}_G\dot{\theta} \\ =&\ T(1-t) - R + X'_{F.K.}(\zeta_G,\phi,\theta,\psi) \\ &-(1-t_R)F_N\sin\delta \\ (m+m_y)\dot{V} &+ Y_V V + m_y x_G\ddot{\psi} + (m+m_x)U\dot{\psi} \\ &-Y_{\dot{\psi}}\,\dot{\psi} - m_y z_G\ddot{\phi} \\ =&\ Y'_{F.K.}(\zeta_G,\phi,\theta,\psi) + Y_{D.F.}(\dot{\eta}_w,\ddot{\eta}_w) \\ &-(1+a_H)F_N\cos\delta \\ (m+m_z)\ddot{\zeta}_G &+ Z_{\dot{\zeta}_G}\dot{\zeta}_G - Z_{\ddot{\theta}}\,\ddot{\theta} + Z_{\dot{\theta}}\,\dot{\theta} \\ &+Z_\theta\theta - m_y z_G\dot{\phi}^2 \\ =&\ Z'_{F.K.}(\zeta_G,\phi,\theta,\psi) + Z_{D.F.}(\dot{\zeta}_w,\ddot{\zeta}_w) \\ &+mg \end{aligned} \qquad (3)$$

Rotational Motions And Moments

$$\begin{aligned}(I_{xx}+J_{xx})\ddot{\phi} &+ K_{\dot{\phi}}\,\dot{\phi} - (I_{xx}+J_{xx})\dot{\theta}\,\dot{\psi} \\ &-m_x z_G U\dot{\psi} - m_y z_G\dot{V} - (Y_V V - Y_{\dot{\psi}}\dot{\psi})z_G \\ =&\ K'_{F.K.}(\zeta_G,\phi,\theta,\psi) + (1+a_H)h_R F_N\cos\delta \\ (I_{yy}+J_{yy})\ddot{\theta} &+ M_{\dot{\theta}}\dot{\theta} - M_\theta\theta - M_{\ddot{\zeta}_G}\ddot{\zeta}_G - M_{\dot{\zeta}_G}\dot{\zeta}_G \\ &+m_x z_G\dot{U} + (I_{xx}+J_{xx})\dot{\phi}\,\dot{\psi} \\ =&\ M'_{F.K.}(\zeta_G,\phi,\theta,\psi) + M_{D.F.}(\dot{\zeta}_w,\ddot{\zeta}_w) \\ (I_{zz}+J_{zz})\ddot{\psi} &+ (N_{\dot{\psi}} + m_y x_G U)\dot{\psi} + m_y x_G\dot{V} \\ &+N_V V - (I_{xx}+J_{xx})\dot{\theta}\,\dot{\phi} - m_y z_G U\dot{\phi} \\ =&\ N'_{F.K.}(\zeta_G,\phi,\theta,\psi) + N_{D.F.}(\dot{\eta}_w,\ddot{\eta}_w) \\ &+(1+a_N)l_R F_N\cos\delta \end{aligned} \qquad (4)$$

where m is the mass of ship, m_x, m_y and m_z the added mass with respect to the x, y and z axes directions, I_{xx}, I_{yy} and I_{zz} the moments of inertia about x, y and z axes, J_{xx}, J_{yy} and J_{zz} the added moments of inertia, x_G and z_G the displacement of added mass center with respect to the origin of the coordinate system fixed in the center of gravity of the ship, U, V and W the velocities along the x', y' and z' axes, and $\dot{\phi}$, $\dot{\theta}$ and $\dot{\psi}$ the angular velocities about the x', y' and z' axes, T the thrust of propeller, t the thrust deduction, and R ship resistance, $Z_{\dot{\zeta}_G}$, $Z_{\ddot{\theta}}$, $Z_{\dot{\theta}}$, Z_θ, $M_{\dot{\theta}}$, M_θ, $M_{\ddot{\zeta}_G}$ and $M_{\dot{\zeta}_G}$ the hydrodynamic coefficients for seakeeping motion[7], $X_{V\dot{\psi}}$[22], $Y_V, Y_{\dot{\psi}}, N_V$ and $N_{\dot{\psi}}$[14] are the hydrodynamic derivatives for manoeuvring motion, $K_{\dot{\phi}}$ the damping coefficient of rolling[4], t_R correction factor of resistance due to steering, a_H coefficient of interaction of rudder normal force on side force, a_N coefficient of interaction of rudder force on yaw moment, l_R horizontal distance between rudder and C.G. of the ship, F_N normal force on rudder[22], $X'_{F.K}$, $Y'_{F.K}$ and $Z'_{F.K}$ Froude-Krylov forces[28], $K'_{F.K}$, $M'_{F.K}$ and $N'_{F.K}$ Froude-Krylov moments[28], $Y_{D.F}$, $Z_{D.F}$ and $M_{D.F}$, $N_{D.F}$ the diffraction forces and moments[7].

Hydrodynamic Coefficients for Seakeeping and Manoeuvring Motions

$$\begin{aligned} Z_{\dot{\zeta}_G} &= \int_L N_z(x)\,dx \\ Z_{\ddot{\theta}} &= \int_L m_z(x)x\,dx \\ Z_{\dot{\theta}} &= -\int_L N_z(x)x\,dx + (m_z - m_x)U \\ Z_\theta &= U\int_L N_z(x)dx \\ M_{\dot{\theta}} &= \int_L N_z(x)x^2\,dx \\ M_\theta &= U\int_L N_z(x)x\,dx \\ M_{\ddot{\zeta}_G} &= m_z x_G \\ M_{\dot{\zeta}_G} &= \int_L N_z(x)\,dx + (m_z - m_x)U \\ K_{\dot{\phi}} &= 2\alpha_e(I_{xx}+J_{xx})[1+0.8(1-e^{-10F_n})] \end{aligned} \qquad (5)$$

$$\begin{aligned} Y_V &= \frac{1}{2}\rho L d U\left[\frac{\pi}{2}\left(\frac{2d}{L}\right) + 1.4C_B\frac{B}{L}\right] \\ N_V &= \frac{1}{2}\rho L^2 d U\left(\frac{2d}{L}\right) \\ Y_{\dot{\psi}} &= \frac{1}{2}\rho L^2 d U\left[\frac{\pi}{4}\left(\frac{2d}{L}\right)\right] \\ N_{\dot{\psi}} &= \frac{1}{2}\rho L^3 d U\left[\frac{2d}{L}\left(0.54 - \frac{2d}{L}\right)\right] \end{aligned} \qquad (6)$$

where $N_z(x)$ is the wave damping coefficient of Lewis form section[4,7], $m_z(x)$ the added mass of Lewis form section, L, B and d the ship length, breadth and draft, C_B the block coefficient of ship.

Rudder Force

$$F_N = \frac{1}{2}\rho A_R f_\alpha U_R^2 \sin\alpha_R \qquad (7)$$

where A_R is the rudder area, U_R and α_R effective inflow velocity and angle to rudder, f_α normal force coefficient of rudder force, δ rudder angle.

Froude–Krylov Forces and Moments

$$\begin{aligned} X'_{F.K}(\zeta_G,\phi,\theta,\psi) &\cong -\rho g\cos\chi \\ &\times\int_L F(x)A(x)\sin k(\xi_G + x\cos\chi - ct)dx \end{aligned}$$

$$Y'_{F.K}(\zeta_G,\phi,\theta,\psi) \cong \rho g \sin\chi$$
$$\times \int_L F(x)A(x)\sin k(\xi_G + x\cos\chi - ct)\mathrm{d}x$$
$$Z'_{F.K}(\zeta_G,\phi,\theta,\psi) \cong -\rho g \int_L A(x)\mathrm{d}x$$
$$-\rho g \int_L F(x)A(x)\cos k(\xi_G + x\cos\chi - ct)\mathrm{d}x$$
$$K'_{F.K}(\zeta_G,\phi,\theta,\psi) \cong$$
$$-\rho g \int_L (y_{B(x)}\cos\phi - z_{B(x)}\sin\phi)A(x)\mathrm{d}x$$
$$-\rho g \sin\chi \int_L (z_{B(x)}\cos\phi + y_{B(x)}\sin\phi)$$
$$\times F(x)A(x)\sin k(\xi_G + x\cos\chi - ct)\mathrm{d}x$$
$$M'_{F.K}(\zeta_G,\phi,\theta,\psi) \cong \rho g \int_L xA(x)\mathrm{d}x$$
$$+\rho g \int_L xF(x)A(x)\cos k(\xi_G + x\cos\chi - ct)\mathrm{d}x$$
$$N'_{F.K}(\zeta_G,\phi,\theta,\psi) \cong \rho g \sin\chi$$
$$\times \int_L xF(x)A(x)\sin k(\xi_G + x\cos\chi - ct)\mathrm{d}x \quad (8)$$

where $A(x)$ is the instantaneously immersed area of ship section, ξ_G the relative position of ship to waves, χ the heading angle of ship to wave, c the phase velocity of waves, $y_{B(x)}$ and $z_{B(x)}$ the center of buoyancy, $\dot{\zeta}_w$ and $\dot{\eta}_w$ are the velocities of orbital motion with respect to y and z axes, ζ_w a sinusoidal wave at any time and at the position x, y, and z written as

$$\begin{aligned}\zeta_w \;=\; & -\zeta_G + x\theta + a\cos k[\xi_G + x\cos\chi \\ & -(y\cos\phi - z\sin\phi)\sin\chi - ct]\end{aligned} \quad (9)$$

and $F(x)$ coefficient of pressure gradient of waves given as

$$F(x) = ak\frac{\sin(k\frac{B(x)}{2}\sin\chi)}{k\frac{B(x)}{2}\sin\chi}e^{-k\{\zeta_G + d(x)\}} \quad (10)$$

Diffraction Forces and Moments

$$Y'_{D.F.}(\dot{\eta}_w,\ddot{\eta}_w) = g\sin\chi \int_L m_y(x)F(x)\sin k(\xi_G$$
$$+x\cos\chi - ct)\mathrm{d}x$$
$$+c\sin\chi \int_L N_y(x)F(x)\cos k(\xi_G$$
$$+x\cos\chi - ct)\mathrm{d}x$$
$$Z'_{D.F.}(\dot{\zeta}_w,\ddot{\zeta}_w)$$
$$= -g \int_L m_z(x)F(x)\cos k(\xi_G + x\cos\chi - ct)\mathrm{d}x$$
$$+c \int_L N_z(x)F(x)\sin k(\xi_G + x\cos\chi - ct)\mathrm{d}x$$
$$M'_{D.F.}(\dot{\zeta}_w,\ddot{\zeta}_w)$$
$$= g \int_L m_z(x)F(x)x\cos k(\xi_G + x\cos\chi - ct)\mathrm{d}x$$
$$-c \int_L N_z(x)F(x)x\sin k(\xi_G + x\cos\chi - ct)\mathrm{d}x$$
$$N'_{D.F.}(\dot{\eta}_w,\ddot{\eta}_w) = g\sin\chi \int_L m_y(x)F(x)x\sin k(\xi_G$$
$$+x\cos\chi - ct)\mathrm{d}x$$
$$+c\sin\chi \int_L N_y(x)F(x)x\cos k(\xi_G$$
$$+x\cos\chi - ct)\mathrm{d}x \quad (11)$$

4. NUMERICAL EXPERIMENTS

In order to find out the critical metacentric height and waves leading up to extreme motion and capsizing of the container ship mentioned in the previous section by solving the equations of coupled six degrees of freedom, numerical experiments were conducted. For the computation, a standard numerical procedure is employed to integrate the equations of motion leading to a step-by-step approximation of ship motion.

Effects of Wave to Ship Length Ratio

At first , numerical experiments in time domain were conducted for the ship running at the heading angles of 0, 30 and 60 degrees to waves. Fig.9 is the examples of the time histories of yawing, pitching and rolling in case of GM=0.8(m) and ship-wave velocity ratio U/c=0.7. Fig.10 stands for the results of numerical experiment of the critical GM leading up to capsize against wave-ship length ratio λ/L.

It is an interesting point whether the critical GM is larger or smaller than the GM=0.92m designed to satisfy the weather criteria A562. The ship is safe in the critical GM smaller than designed GM. The ship will be unsafe in the range of waves λ/L = 1.25 to 1.5 having the heading angle equal to zero and in the waves of λ/L = 1.25 to 1.75 having the heading angles equal to 30 degrees.

Effects of Wave Height to Length Ratio

Fig.11 indicates the result of numerical experiments to find out the critical GM with respect to the wave height to length ratio H/λ. The ship will be unsafe in the wave height larger than $H/\lambda = 1/20$.

Effects of Heading Angles of Ship to Wave

Fig.12 shows the results of numerical experiments to find out the critical GM with respect to the heading angles of ship to waves of λ/L = 1.0 and 1.5. The ship will be safe for any heading angles in the wave

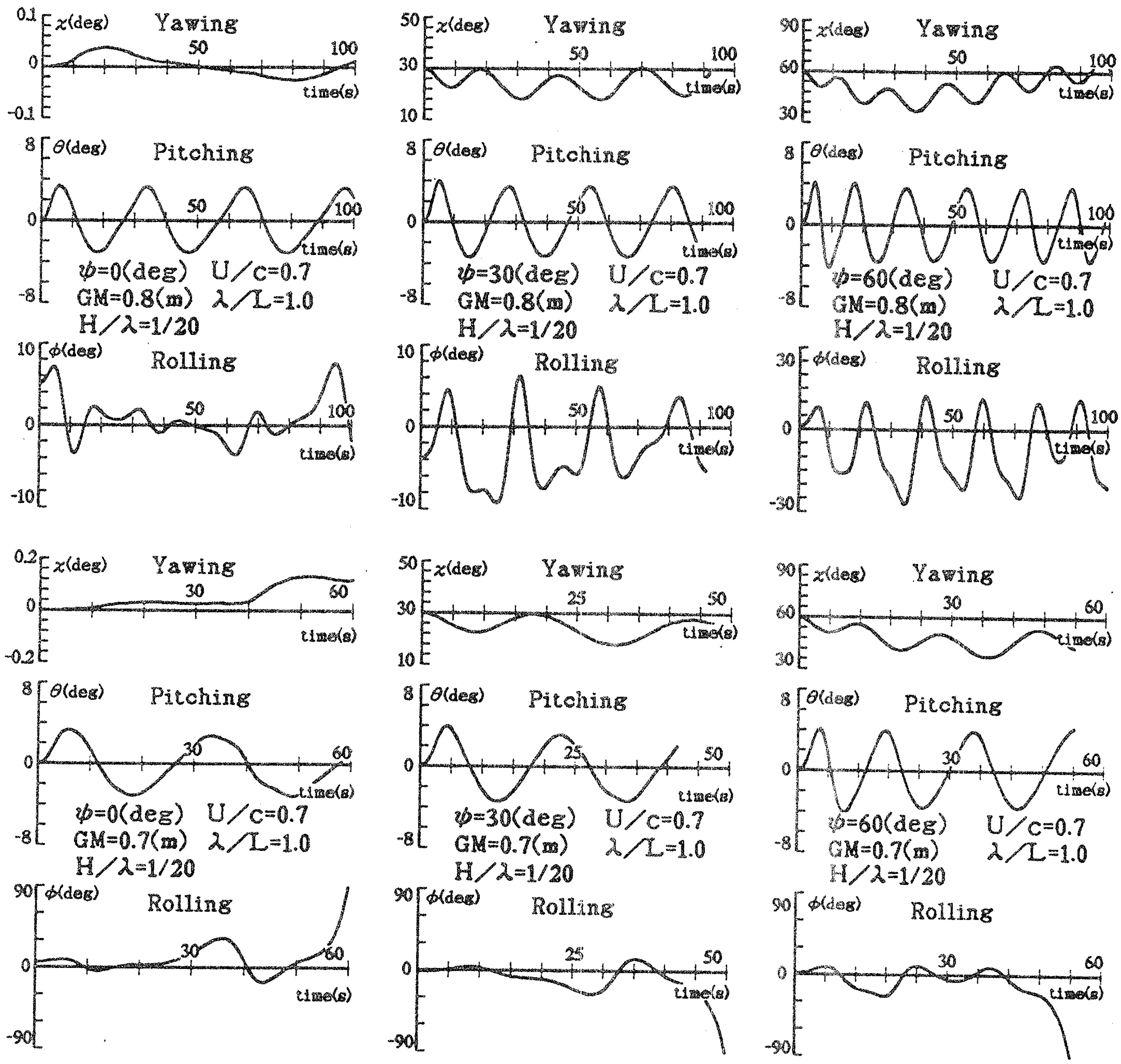

Fig.9 Time histories of ship motion in following waves of $\lambda/L=1$

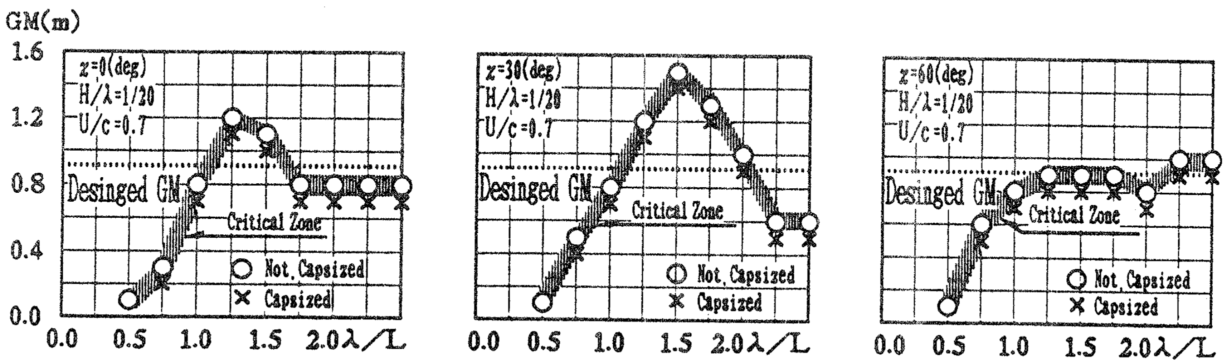

Fig.10 Critical metacentric height leading up to capsize versus λ/L

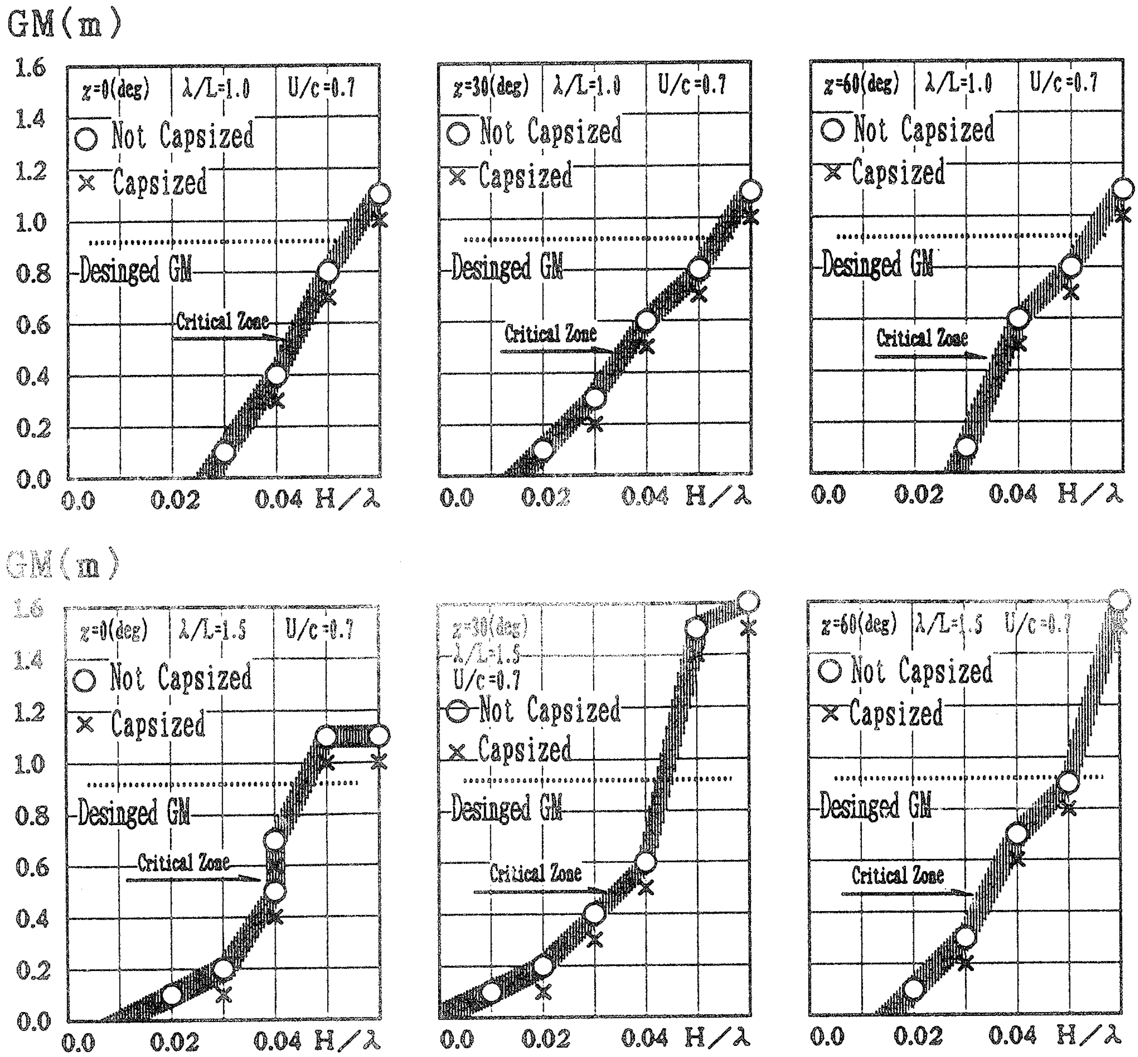

Fig.11 Critical metacentric height leading up to capsize versus H/λ

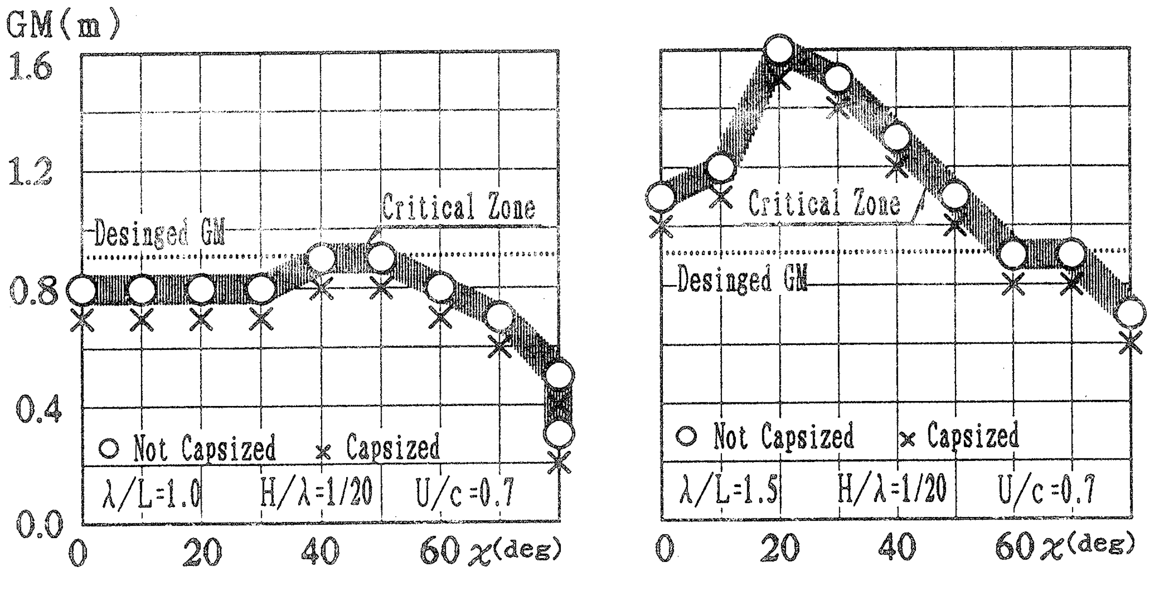

Fig.12 Critical metacentric height leading up to capsize versus heading angle of a ship to waves

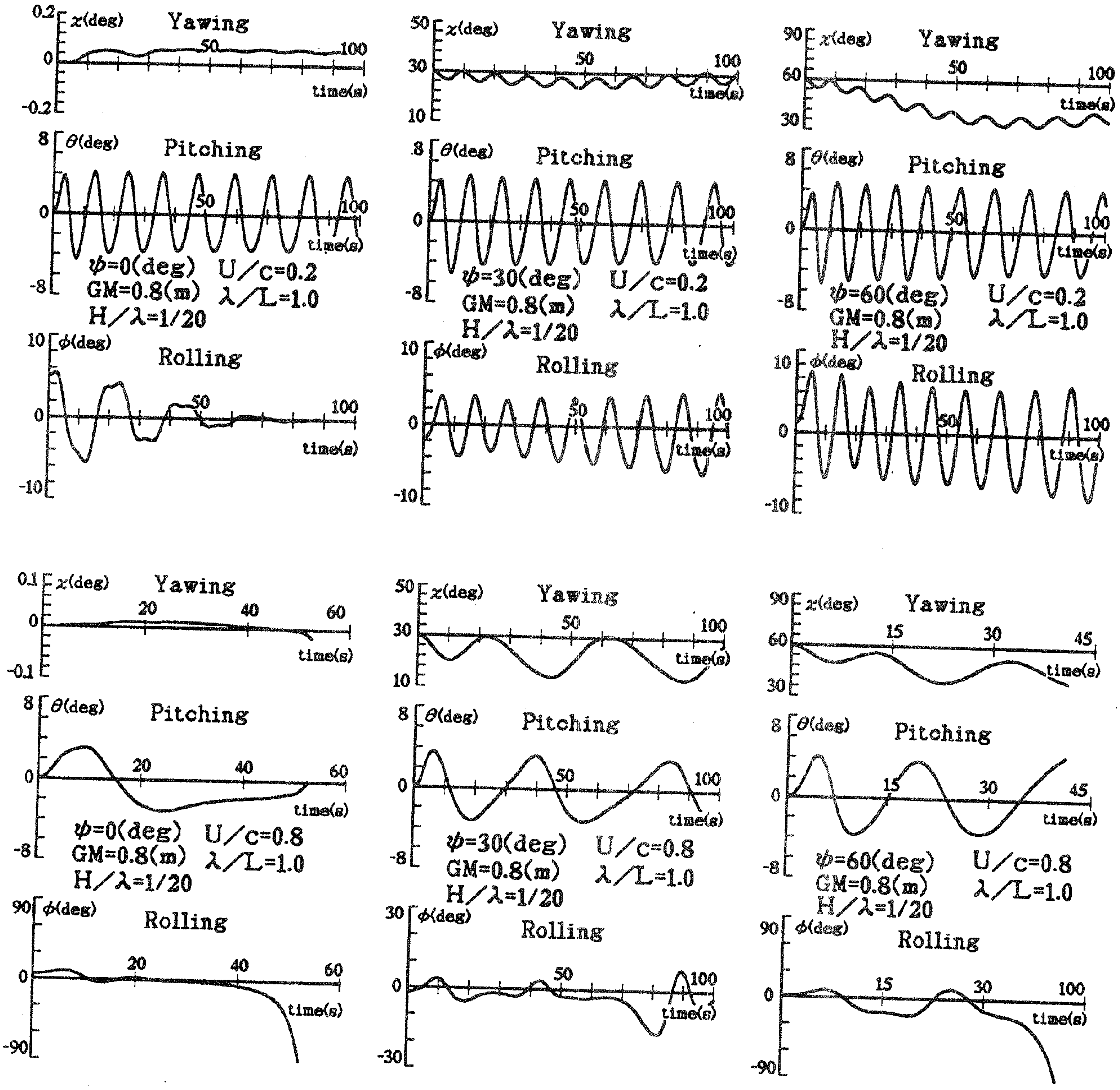

Fig.13 Time histories of ship motion in following and quartering waves of $\lambda/L=1$

of $\lambda/L = 1.0$ but unsafe for the heading angles from zero to 50 degrees in the wave of $\lambda/L = 1.5$.

Effects of Ship to Wave Velocity Ratio

Finally, numerical experiments in time domain were conducted for the ship running at the lower and higher speeds. Fig.13 are the examples of the time histories of yawing, pitching and rolling. The ship will be safe in the case of $U/c = 0.2$ but unsafe in the case of $U/c = 0.8$ for the heading angles of zero and 60 degrees. Fig.14 indicates the results of numerical experiment to find out the critical GM with respect to U/c.

The capsize is seen to be related to pure loss of stability when a crest moves amidships at the speed nearly equal to the ship for a sufficient length of time to capsize. The wave length would be of about the same length as the ship.

5. CONCLUSIONS

This paper provides an analytical approach to ship motion and capsizing in extreme quartering seas. The problem is divided into the effects of waves on the hydrostatics of sway motion. First, the hydrostatic indices, GM, GZ and E are evaluated up to taking

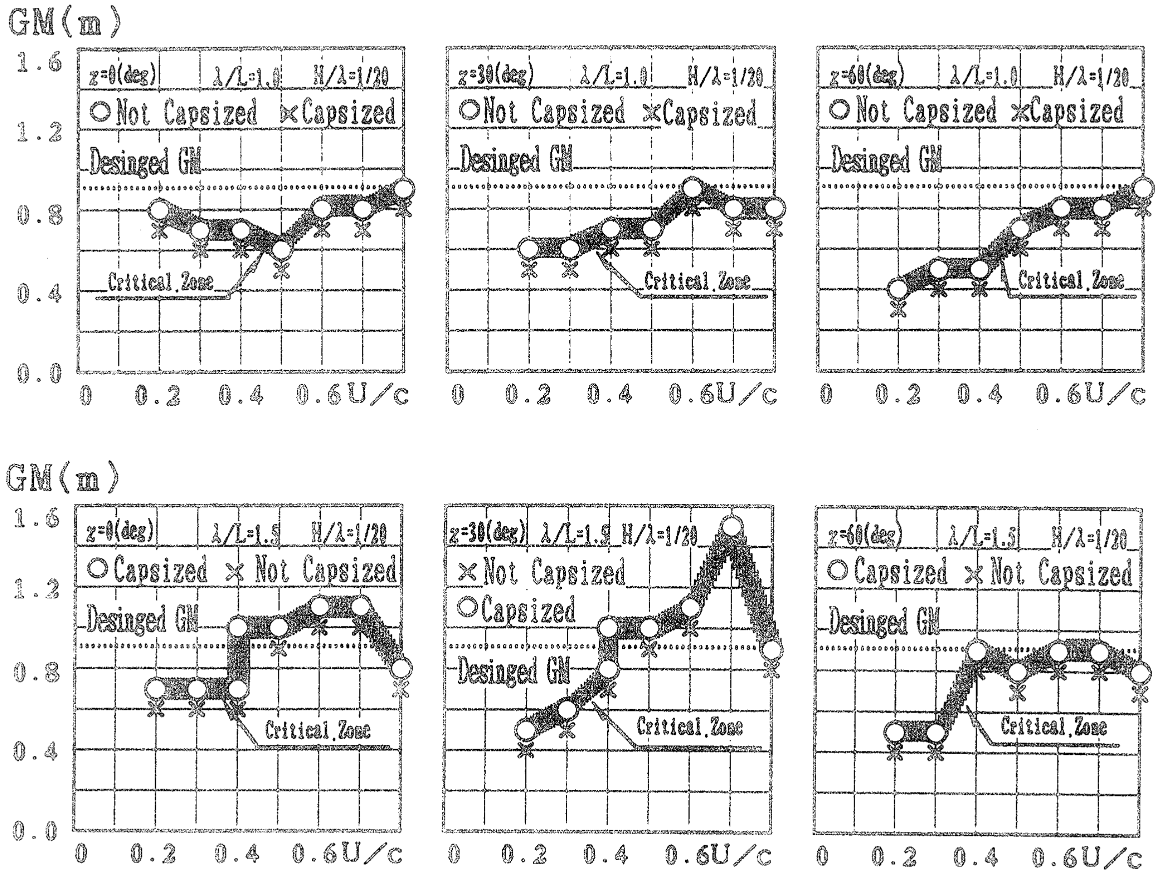

Fig.14 Critical metacentric height leading up to capsize versus U/c

into account the effects of the relative position of ship to waves, the heading angles, wave height and length. Next, a mathematical model is proposed on the basis of Froude–Krylov forces taking into account the instantaneous free surface at each time instant and linearized hydrodynamic forces on ship hull. Finally, using the mathematical model, a lot of numerical experiments are conducted in order to find out the extreme wave and ship motion leading up to capsizing. The results of numerical experiments are presented and discussed for the critical metacentric height with respect to the several parameters.

Some of the main findings are the importance of the critical GM leading up to capsize in extreme quartering seas. The critical GM seams to be larger than the GM designed to satisfy the criteria A562 in beam sea and wind. It will be a considerable problem for the safety of ship at sea how to determine a reasonable GM and how to operate a ship in extreme quartering seas. The critical GM is related to the reduction of GZ at wave crest amidships and the reduction is largely dependent on the flare configuration, free boad of a ship and the size of waves. So that it is an important implication to consider the dangerous wave size on the basis of the risk analysis.

REFERENCES

1) Watanabe, Y., On the Dynamic Properties of the Transverse Instability of a Ship due to Pitchings, J. of Soc. of Naval Arch., Vol. 53, 1934.

2) Grim, O., Rollschwingungen, Stabilitat und Sich heit im Seegang, Schiffistechnik, 1952.

3) Kerwin, J.E., Notes on Roll in Longitudinal Wave I.S.P., Vol.2 (16), 1955.

4) Motora, S., On the Measurement of Added Mass and Added Moment of Inertia for Ship Motion, J. of Soc. of Naval Arch., Vol. 105–107, 1959, 1960.

5) Paulling, J.R., The Transverse Stability of a Ship in a Longitudinal Seaway, J. of Ship Research, SNAME, Vol.4, No.4, March, 1961.

6) Grim O., Beitrag zu dem Problem der Sicherheit des Schiffes in Seegang, Schiff und hafen, helt 6, 1961.

7) Tasai, F., Damping Force and Added Mass of Ships Heaving and Pitching (Continued), Trans. of the West-Japan Soc. of Naval Arch., Vol.21, 1961.

8) Du Cane, P., Goodrich, G.J., The Following Sea, Broaching and Surging, Trans. RINA, Vol.104, April, 1962.

9) Takahashi, T., Mechanism of Rolling and Application,(in Japanse), Report of Mitsubishi Heavy Industry Nagasaki Technical Institute, No.2842, 1969, Unpublished.

10) Boses, P., Steuern eines Shiffes im Schweren Achterlichen Seegange, J.S.T.G., Bd, 1971.

11) Price, W.G., The Stability of Ship in a Simple Sinusoidal Wave, J. of Mechanical Engineering Science, Vol.14, 1972.

12) Chou, S.J., Oakely, O.H., Paulling, J.R., Van Slyke, R., Wood, P.D., Zink, P.F., Ship Motions and Capsizing in Astern Seas, Dep. of Transportation United States Coast Guard, Rep. No. CG-D-103-75, 1974.

13) Paulling, J.R., Oakley, and Wood, P.A. "Ship Capsizing in Heavy Seas: The Correlation of Theory and Experiments". International Conference on Stability of Ships and Ocean Vehicles. University of Strathclyde, 1975.

14) Inoue, S., Kijima, K. and Moriyama,F., "Presumption of Hydrodynamic Derivatives on Ship Manoeuvring in Trimmed Condition" Trans. of West–Japan Society of Naval Architects. No. 55, March 1978.

15) Renilson, M.R., Driscoll, A., Broaching-An Investigation into the Loss of Directional Control in Severe Following Seas, Spring Meeting RINA, 1981.

16) Motora, S., Fujino, M., Fuwa, T., On the Mechanism of Broaching-to Phenomena, STABILITY 1982.

17) Hamamoto, M., Nomoto, K., Transverse Stability of Ship in a Following Sea, STABILITY'82, 1982.

18) Kuo, C., Vassalos, D., The Stratchclyde Approach to Practical Ship Stability Criteria, Work shop on Stability, Germanisch Lloyd, 1984.

19) Safety and Stability of Ship and Offshore Structures – Third Marine Dynamics Symposium, October, 1986.

20) Hamamoto, M., Transverse Stability of Ship in a Quartering Sea, STABILITY'86, 1986.

21) Ohkusu, M., Prediction of Wave Forces in a Ship Running in a Following Waves with Very Low Encounter Frequency, J. of Soc. of Naval Arch. Vol.159, 1986.

22) Prediction of Ship Manoeuverability and its Applications, 4th Marine Dynamics Symposium, 1987.

23) Hamamoto, M., Akiyoshi, T., Study on Ship Motions and Capsizing in Following Seas (1st Report), J. of Soc. of Naval Arch. Vol.163, 1988.

24) Hamamoto, M., Shirai, T., Study on Ship Motions and Capsizing in Following Seas (2nd Report), J. of Soc. of Naval Arch. Vol.165, 1989.

25) de Kat J. O. , Paulling J. R. , The Simulation of Ship Motions and Capsizing in Severe Seas, Trans. SNAME, 1989.

26) Kan, M., Saruta, T., Taguchi, H., Yasuno, M., Takaishi, Y., Model Tests on Capsizing of a Ship in Quartering Waves, STABILITY'90, 1990.

27) Hamamoto, M., Shirai, T., Wakiyama, N., An Analytical Approach to Capsizing of a Ship in Following Seas, STABILITY'90, 1990.

28) Umeda, N., Probabilistic Study on Surfriding of a Ship in Irregular Following Seas, STABILITY'90, 1990.

29) Hamamoto, M., Kim, Y.S., Uwatoko, K., Study on Ship Motions and Capsizing in Following Seas (Final Report), J. of Soc. of Naval Arch. Vol.170, 1991.

30) Hamamoto, M., Tsukasa, Y., An Analysis of Side Force and Yaw Moment on a Ship in Quartering Waves, J. of Soc. of Naval Arch. Vol.171, 1992.